We are IntechOpen,
the world's leading publisher of
Open Access books
Built by scientists, for scientists

4,800
Open access books available

122,000
International authors and editors

135M
Downloads

Our authors are among the

154
Countries delivered to

TOP 1%
most cited scientists

12.2%
Contributors from top 500 universities

CLARIVATE ANALYTICS
BOOK CITATION INDEX
INDEXED

WEB OF SCIENCE™

Selection of our books indexed in the Book Citation Index
in Web of Science™ Core Collection (BKCI)

Interested in publishing with us?
Contact book.department@intechopen.com

High-Speed and High-Precision Position Control Using a Nonlinear Compensator

Kazuhiro Tsuruta[1], Kazuya Sato[2] and Takashi Fujimoto[1]
[1]Kyushu Sangyo University
[2]Saga University
Japan

1. Introduction

To achieve high-speed, high-precision position control for semiconductor product machines and industrial robots, it is well known that PID control is widely applied (Kojima, T., 2004). Many PID control methods have been proposed for such a system so far. In general, proportional position control and proportional plus integral velocity control or integral plus proportional velocity control (P,PI/I-P), which is a type of proportional plus integral plus deferential control (PID), is applied in many industrial applications in Japan. However, the parameters of the control of P,PI/I-P must be changed to maintain a good motion performance when the characteristic of the control target change. As a method to compensate for a change of the control target, a disturbance observer is proposed (Ohishi, K. et al., 1999). Using this method, a load disturbance force is estimated based on a model set beforehand and adds an estimated disturbance force to a control input. However, it might cause the deterioration of the control performance when a control target model is different from real control target greatly. Furthermore, it is difficult to get a correct model because a lot of nonlinear elements such as the friction may change in control target in time and environment (Canudas-de-Wit, C. et al., 1995; Lischinsky, P. et al., 1999; Futami, S. et al., 1990; Otsuka, J. & Masuda, T., 1998; Iwasaki, M. et al., 2000; Tsuruta, K. et al., 2000, 2003). In addition, based on a control target model estimated in real time, the method to change the several control parameters is proposed to compensate it for a change of the control target (Kuwon, T. et al., 2006), but might cause the deterioration of the control response under the influence of an estimate error. Therefore, adaptive control (Suzuki, T., 2001; Sato, K. et al., 2005, 2006, 2007, 2008) and sliding mode control (Nonami, K. & Den, H., 1994; Utkin, V, I., 1977; Harashima, F. & Hashimoto, H., 1986; Fujimoto, T. et al., 2006) are given to solve these problems. However, that is hard to understand these methods to the engineer who got used to PID control; have a problem. In this chapter, we propose a new P,PI/I-P control method that includes a nonlinear compensator, that it is easy to understand for a PID control designer. The control objective is to get a high-speed and high-precision positioning response regardless of the case of control references or load characteristics change. The algorithm of the nonlinear compensator is based on sliding mode control with chattering compensation. The effectiveness of the proposed control method is evaluated with three kinds of single-axis slide system experimentally. The first experiment system is two slider tables comprised of an AC servo motor, a coupling and a ball-screw, the second one is a

slide table using an AC linear motor and the third one is a slide table using synchronous piezoelectric device driver (Egashira, Y. et al., 2002; Kosaka, K. et al., 2006). By the first experiments, it is evaluated using single-axis slide system comprised of full closed feedback via point-to-point control response and tracking control response when load characteristics of the control target change. By the second experiments, it is evaluated using a linear motor driven slider system via tracking control at low-velocity, and the resolution of this system is 10nm. By the third experiments, it is evaluated a stepping motion and tracking motion using a synchronous piezoelectric device driver. Then, we derive control algorithm with nonlinear compensator and describe each experimental results.

2. Control method

In this section, we describe a P,PI/I-P+FF control method and propose the P,PI/I-P+FF control method with nonlinear compensator. The control objective is to design a control input to track a given position reference.

2.1 Conventional P,PI/I-P+FF control method

In general, P,PI/I-P control method is applied in many industrial applications. To achieve high-speed positioning response, velocity feed-forward compensation (FF) is usually applied. The FF compensation is effective in compensating it for a response delay of the positioning. As for P,PI/I-P method, positioning and velocity control are comprised of cascade control. When we do not make positioning, we can control velocity by inputting a direct velocity reference. Fig. 1 shows a block diagram of P,PI/I-P+FF control method. In this figure, a signal x_d is position reference, a signal x is table position, a signal $\dot{x}$ is table velocity, a signal e_1 is position error, a signal e_2 is velocity error and a signal u is control input which means torque command, respectively. Here, the differentiation uses backward difference equation. K_p is position loop gain, K_i is velocity integral gain, K_v is velocity loop gain, α is velocity feed-forward gain, β is the change fixed number to change velocity PI control method or velocity I-P control method. If β is 1, the velocity control is I-P control method, else if β is 0, the velocity control is PI control method. K_f is the torque conversion fixed number. The symbol s is Laplace transfer operator, s means differentiator and $1/s$ means integrator.
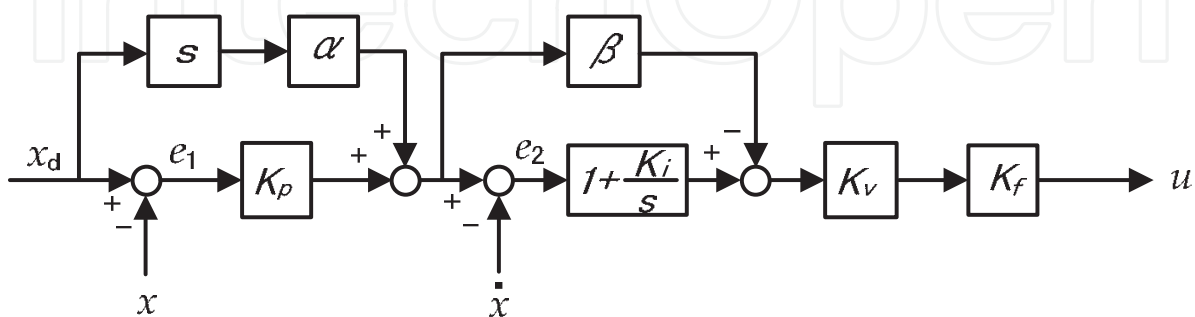

Fig. 1. Block diagram of P,PI/I-P+FF control method.

The control input u is given as follows

$$u = K_v K_f \left\{ \left(1 + \frac{K_i}{s}\right) e_2 - \beta\left(K_p e_1 + \alpha\dot{x}_d\right) \right\} \tag{1}$$

2.2 Proposed control method

In this paper, we will design a PID+FF controller with a nonlinear compensator for high accuracy and a fast response with small overshoot. Fig. 2 shows a block diagram of the P,PI/I-P+FF control method with proposed compensator. The algorithm of the nonlinear friction compensator will be given.
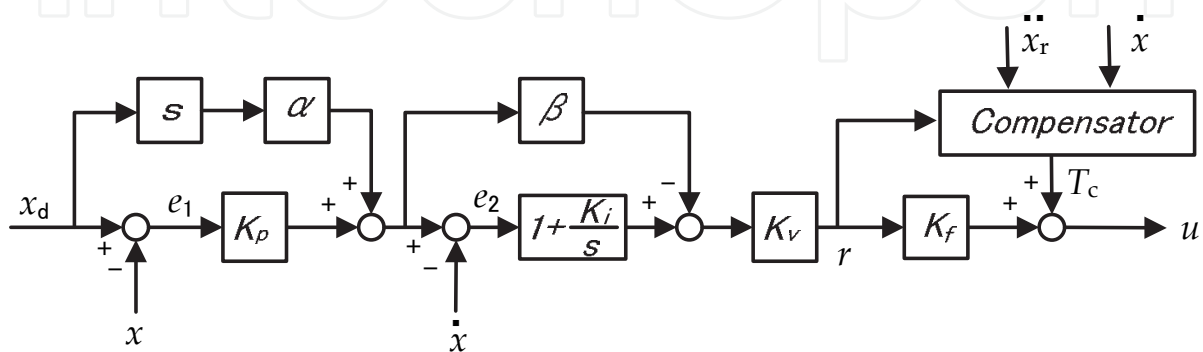

Fig. 2. Block diagram of proposed control method.

The dynamic equation of positioning table can be modelled as follows

$$J\ddot{x} + D\dot{x} + F = u \tag{2}$$

where J is the inertia, D is the viscous friction coefficient, F is the constant disturbance force, x is table position , $\dot{x}$ is table velocity, and u is the control input. Let the error value be

$$e_1 = x_d - x \tag{3}$$

$$e_2 = K_p e_1 - \dot{x} + \alpha\dot{x}_d \tag{4}$$

Taking the second time derivative of both sides for (4) and substituting it into (2), we have

$$\ddot{x} = K_p\dot{e}_1 + \alpha\ddot{x}_d - \dot{e}_2 \tag{5}$$

$$J(K_p\dot{e}_1 + \alpha\ddot{x}_d - \dot{e}_2) + D\dot{x} + F = u \tag{6}$$

$$J\dot{e}_2 = -u + J(K_p\dot{e}_1 + \alpha\ddot{x}_d) + D\dot{x} + F \tag{7}$$

Now, we can define the new signal as

$$r = K_v \left\{ \left(1 + \frac{K_i}{s}\right) e_2 - \beta\left(K_p e_1 + \alpha\dot{x}_d\right) \right\} \tag{8}$$

Taking the time derivative of both sides for (8) and multiplying J to both sides, we have

$$J\dot{r} = JK_v\dot{e}_2 + JK_vK_ie_2 - J\beta K_pK_v\dot{e}_1 - JK_v\alpha\beta\ddot{x}_d$$
$$= K_v\left(-u + JK_p\dot{e}_1 + J\alpha\ddot{x}_d + D\dot{x} + F\right) + JK_vK_ie_2$$
$$- J\beta K_pK_v\dot{e}_1 - JK_v\alpha\beta\ddot{x}_d$$
$$= -K_vu + K_vD\dot{x} + K_vF + JK_v\alpha\ddot{x}_d(1-\beta)$$
$$+ JK_pK_v\dot{e}_1(1-\beta) + JK_vK_ie_2 \tag{9}$$

We define the augmented signal as

$$\ddot{x}_r = \alpha\ddot{x}_d(1-\beta) + K_p\dot{e}_1(1-\beta) + K_ie_2 \tag{10}$$

Then, (9) can be rewritten as

$$J\dot{r} = -K_vu + JK_v\ddot{x}_r + K_vD\dot{x} + K_vF \tag{11}$$

Now, we give the control input u as

$$u = K_fr + T_c \tag{12}$$

where T_c will be given later. Substituting (12) into (11), we have

$$J\dot{r} = -K_vK_fr - K_vT_c + JK_v\ddot{x}_r + K_vD\dot{x} + K_vF \tag{13}$$

The control input u must be determined that the closed-loop system becomes stable. Analysing the closed loop stability, we give the following positive definite function as

$$V = \frac{1}{2}Jr^2 \tag{14}$$

Taking the time derivative of both sides for (14) and substituting (13), we have

$$\dot{V} = Jr\dot{r} = -K_vK_fr^2 + K_vr\left(J\ddot{x}_r + D\dot{x} + F - T_c\right) \tag{15}$$

To achieve a negative $\dot{V}$, the following inequality must be satisfied

$$K_vr\left(J\ddot{x}_r + D\dot{x} + F - T_c\right) \le 0 \tag{16}$$

Then, if we design T_c as follows

$$T_c = \text{sgn}(r)(J_{\max}|\ddot{x}_r| + D_{\max}|\dot{x}| + F_{\max}) \tag{17}$$

where $J_{\max}$, $D_{\max}$ and $F_{\max}$ are maximum values which are predetermined and known, then inequality (16) is satisfied. This sgn function of r is established by a sliding mode control theory. Therefore, if the control input (12) and (17) is applied, then the closed loop system is stable in meaning of Lyapunov stability theory. However, chattering phenomena may occur, because (17) contains the sgn function of r. To avoid the chattering phenomena, we introduce an approximated function of the sign function as follows

$$u = r + \frac{r}{\delta + |r|}(J_{max}|\ddot{x}_r| + D_{max}|\dot{x}| + F_{max}) \tag{18}$$

where δ is the chattering avoidance parameter. Consequently, if we select sufficiently large values of J_{max}, D_{max} and F_{max} in (18), then the time derivative of (14) is always negative and the control objective is accomplished. The P,PI/I-P+FF control method with nonlinear compensator was derived.

3. Experimental results

In this section, we evaluated positioning responses and tracking responses by three kinds of single-axis slide system experimentally. The first experimental system is two slider tables that consists of an AC servo motor, a coupling and a ball-screw, and the second one is a slide table using an AC linear motor and the third one is a slide table using synchronous piezoelectric device driver.

3.1 A table drive system using AC servo motor with a coupling and a ball-screw
The first experiment system is two slider tables comprised of an AC servo motor, a coupling and a ball-screw.

3.1.1 Experimental system
Fig. 3 shows the experimental setup which consists of the following parts. The control system was implemented using a Pentium IV PC with a D/A converter board and a counter board. The control input was calculated by the controller, and its value was translated into a voltage input for the current amplifier through the D/A board. The positions of the positioning table were measured by a position sensor with a resolution of 50 nm. The sensor's signal was provided as a full-closed feedback signal. The sampling period was 0.25 ms. The table with 5 kg weight was mounted on a driving rail. The total inertia of the moving part of the positioning table was approximately 1.128e-4 kgm². The table was supported by a rolling guide through the coupling that was connected with the motor, and the table was driven by an AC servo motor (SGMAS-02ACA21,Yaskawa Electric. Co., Ltd), a ball-screw lead of 20 mm (KR4620A+540L, THK Co., Ltd). The control parameters were set to K_p=75/s, K_v=377 rad/s, K_i=250 rad/s, α=0.55 or 0.60, β=1 and δ=5. The value of J_{max}, D_{max} and F_{max} were selected as five times of J, D, F of the slide table (there is not a weight) which measured beforehand, respectively.
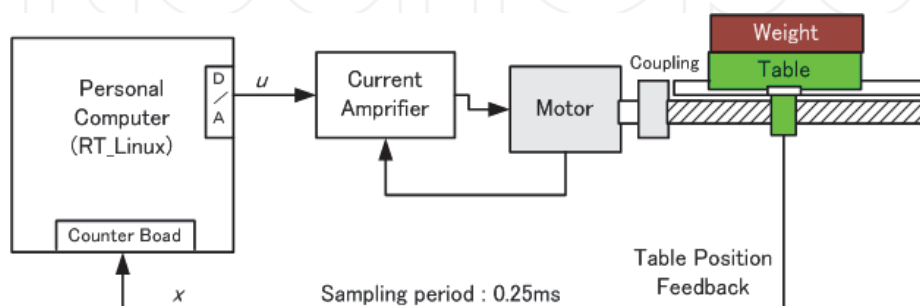

Fig. 3. Experimental system of single axis slider.

Next, the results of positioning responses and tracking responses are shown.

3.1.2 Experimental results

To evaluate our proposed method, we carried out three kinds of experiments. In the first type experiment, it is evaluated that the case of positioning responses when the acceleration/deceleration changes. In the second type of experiment, it is evaluated by the case of positioning responses when the load changes. In the third type of experiment, it is evaluated that the case of tracking responses when the load changes. Fig. 4 shows the experimental table positioning results with the 5 kg-weight in which the positioning reference acceleration/deceleration was changed. The acceleration/deceleration of the first (left side) positioning reference is ±1.0 G, the second is ±1.5 G, the third is ±2.0 G, and the fourth (right side) is ±3.0 G. In this figure, signal ① was the position reference x_d (right side vertical axis), signal ② was the position error (left side vertical axis) using the conventional control method in which the feed-forward gain was set to 0.55, signal ③ was the position error using the conventional control method in which feed-forward gain was set to 0.60, and signal ④ was the position error using the proposed control method in which feed-forward gain was set to 0.55. Fig. 5a shows an expanded graph at 1.0 G and Fig. 5b shows at 3.0 G. In the case of an acceleration/deceleration of 1.0 G, all responses showed approximately the same positioning control performance. However, in the case of an acceleration/deceleration 3.0 G, it is clearly found that there was undesired motion in the form of windup and overshoot using the conventional control methods. On the other hand, there was no windup or overshoot using the proposed control method.
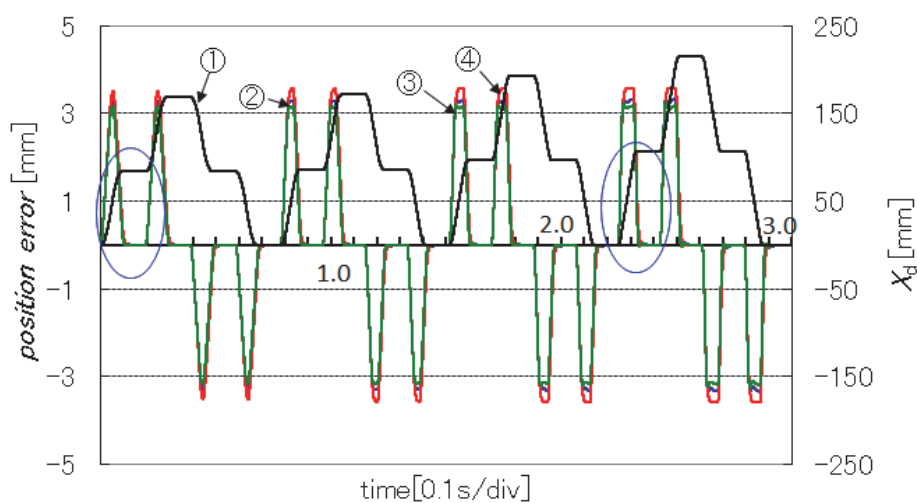

Fig. 4. Position reference and table error.

These results demonstrated the effectiveness of the proposed control method. Generally, it may be said that the acceleration 3.0 G in this experiment is very large because acceleration is used in less than 2.0 G at the ball screw drive table. Fig. 6 shows a torque reference with the conventional control method, and Fig. 7 shows a torque reference (signal ①) and compensated torque T_c (signal ②) with the proposed control method. The rate-torque of the motor is 0.637 Nm, and in both figures, the maximum torque is about 150 % of the rate-torque and is the same value in the conventional method and the proposed method. We found that if a nonlinear compensated torque T_c was very smoothly made, a chattering phenomenon would probably not occur, and we could get a smooth response without any vibration. Fig. 8 shows the response when δ changes in equation (18). In this figure, signal ① is the position reference with an acceleration/deceleration of 3.0 G, ②, ③, and ④ are

the table position errors using the proposed control method, that is, ② with δ=500, ③ with δ=50, and ④ with δ=5. This figure shows the effect of the positioning response when δ changed. These experimental results suggested that we could get the disturbance attenuation performance using nonlinear compensator by changing δ.
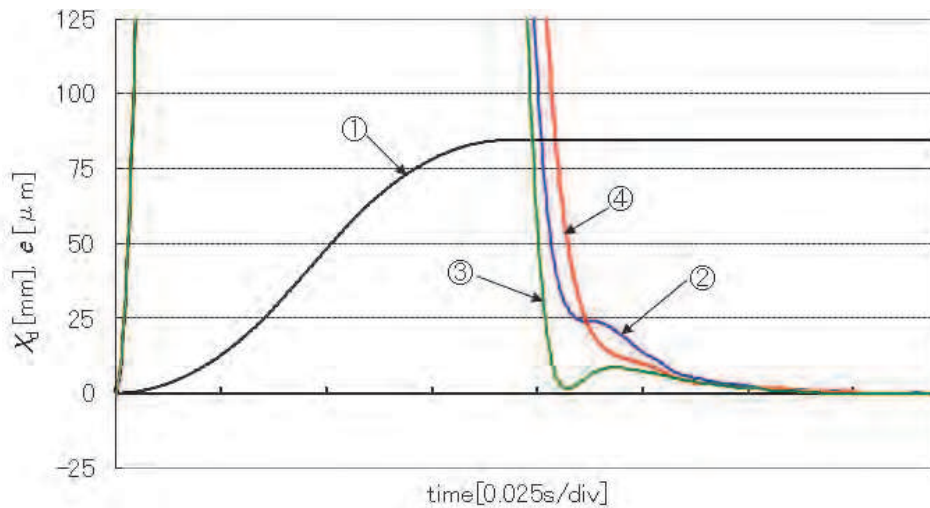

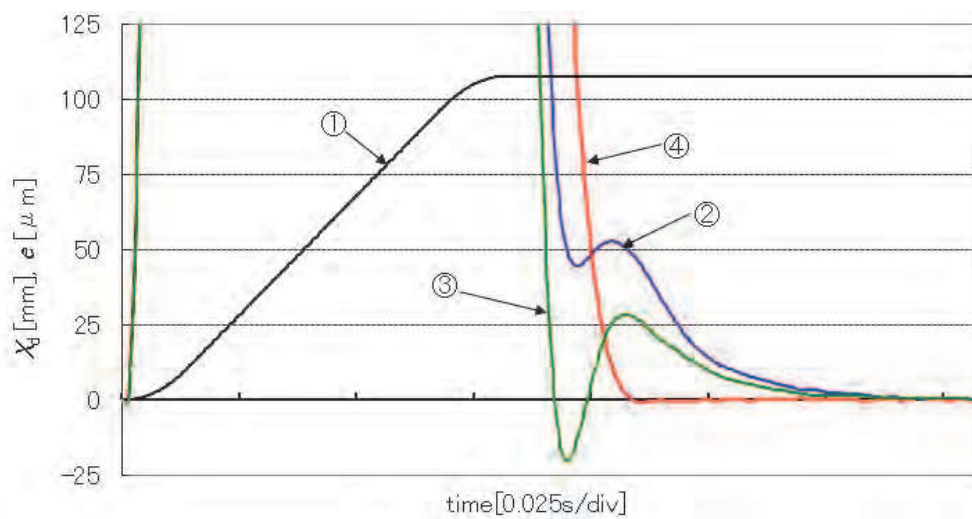Fig. 5a. Experimental results of PTP control (acceleration=1.0 G).
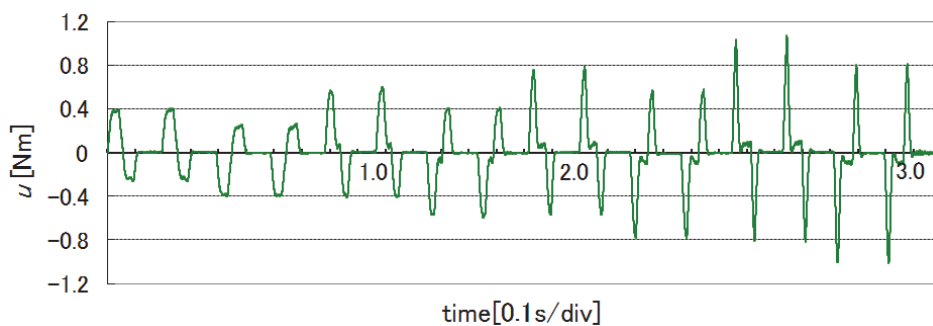

Fig. 5b. Experimental results of PTP control (acceleration=3.0 G).

Fig. 6. Torque reference and compensation torque with the conventional control method.
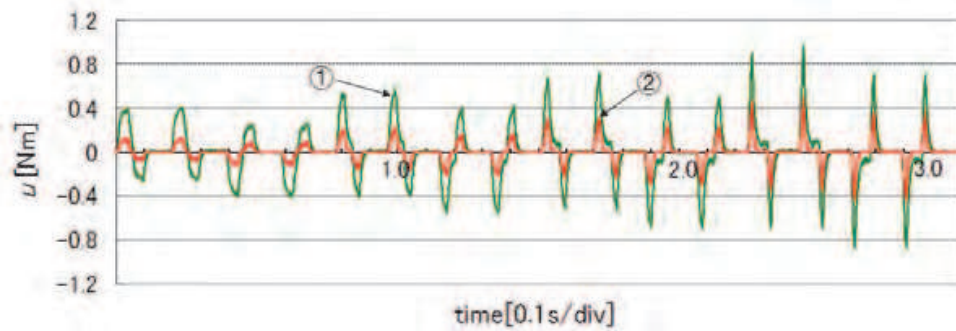
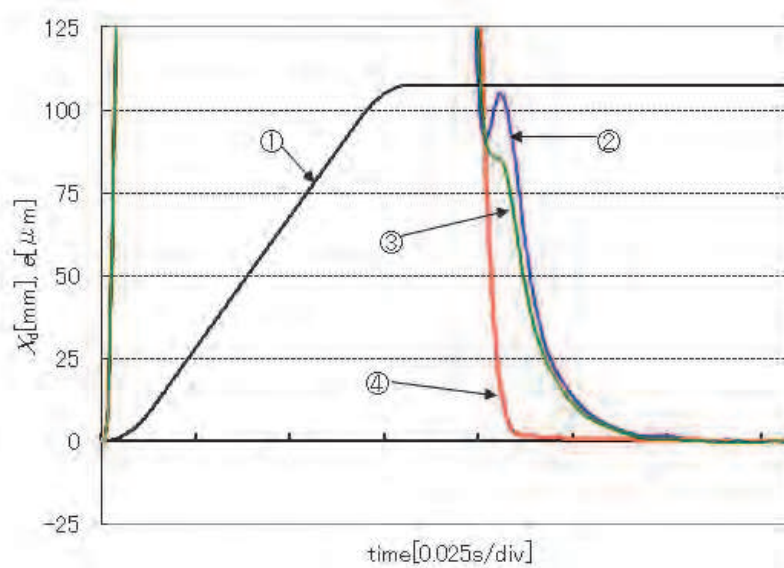Fig. 7. Torque reference and compensation torque with the proposed control method.

Fig. 8. The experimental results of PTP control (δ changed).

In the second type of experiment was a positioning response with load changing. Here, we describe the experimental result that verified the robustness of the proposed control method in the case of real-time load inertia change. To change the load inertia in real time, we prepared two sets of positioning tables, each consisting of a single-axis slider, a coupling, a motor, a servo amplifier, and a linear scale, as shown in Fig. 9. The D/A channel of the torque reference (the voltage) to output through the D/A board from the PC and the counter channel of the table position signal (the pulse) which is entered from the counter board were made to be able to be changed at the same time by the software. Therefore, the weight added or removed, can be imitated, and it is possible to perform the experiment based on the actual mobile status of the production machine. In this experiment, the trapezoid velocity accelerates from zero velocity to 0.4 m/s in 13.5 ms, moving to a max velocity of 0.4 m/s at the constant in 26.75 ms, decelerates to zero velocity in 13.5 ms in Fig. 10 and Fig. 11. The maximum velocity is 0.4m/s by this experiment, but, by the use of the high lead ball screw and the improvement of the frequency response of the counter, can put up the maximum velocity. The present position reference x_d used in the experiment is the value of this trapezoid velocity pattern integrated among at the time, and x_d is the same as the position reference in Fig. 4. The positioning response using the conventional method is shown in Fig. 10, and the positioning response using the proposed method is shown in Fig.

11. In these figures, d_x_d (left side vertical axis) is the position reference differential value which is the trapezoid velocity pattern, d_x (left side vertical axis) is the table velocity, e (right side vertical axis) is the table error of position, and u (right side vertical axis) is the torque reference. The dimension of u % means the ratio for the rating torque. In addition, at 0-200 ms, it is the response with the loop of channel_1 (weight=0 kg), and after 200 ms, it is the response with the loop of channel_2 (weight=5 kg). Incidentally, α=0.60 of the control parameter was the velocity feed-forward gain with the set value shown in section 3.1.1.
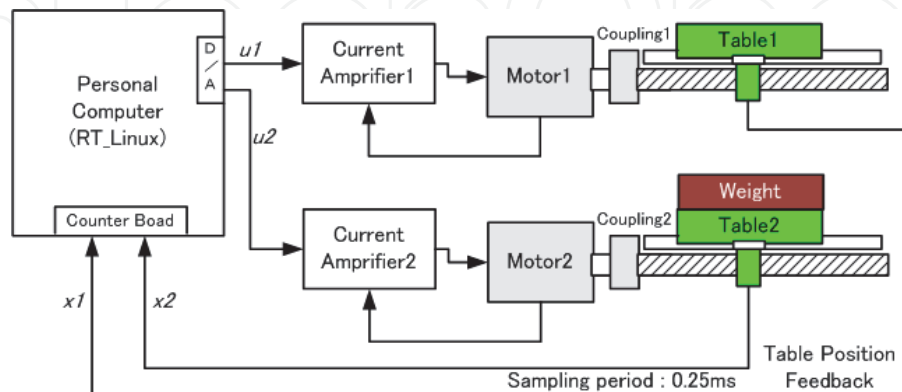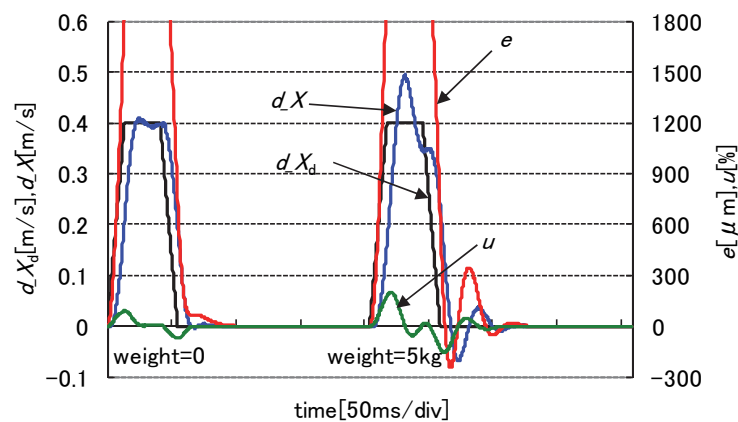

Fig. 9. Experimental system of the load changed.

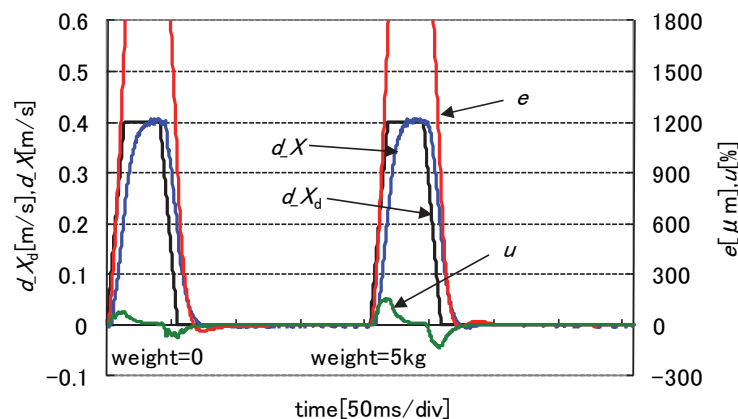Fig. 10. Experimental results of PTP control using the conventional control method.

Fig. 11. Experimental results of PTP control using the proposed control method.

In the result using the conventional method shown in Fig. 10, a windup and a big overshoot occurred in the positioning. This is similar to the unstable phenomenon that occurs in the response of the velocity loop to the position loop when the stability is affected by the velocity loop-gain is becoming small. On the other hand, in the result using the proposed method shown in Fig. 11, there is no windup or overshoot when the weight is increased. Moreover, the torque reference is smoothly made and no vibration occurs. Therefore, as shown in both figures, the high-speed positioning responses following load changes were confirmed when the proposed control method was used.

In the third type of experiment we evaluated the tracking control characteristic when the trapezoid velocity was constant at 13 mm/s or 6.5 mm/s using the single-axis rolling guide slider, as described in section 3.1.1 for a 2-cycle period. There is no weight on the table at 1st period (0-3.6s), and there is 5 kg weight on the table at 2nd period (3.6-7.2s). The result with the 1st period when driving with the conventional control method is shown in Fig. 12 (left side), and the result with the 2nd period is shown in Fig. 12 (right side). Also, the result with the 1st period when driving with the proposed method is shown in Fig. 13 (left side), and the result with the 2nd period is shown in Fig. 13 (right side). In these figures, d_x_d is the position reference differential value, which is the trapezoid velocity pattern, d_x is the table velocity, and e is the table error of position. The control parameters were set to the same values as listed in section 3.1.1, and the velocity feed-forward gain was changed to α=1.0 to improve the tracking control from the set value when evaluating positioning response. In all cases of Figs. 12, 13, the maximum error occurred when the operation was influenced by the initial maximum static friction force, and a large error occurred when the velocity reversal was equivalent to the stroke end of the table.
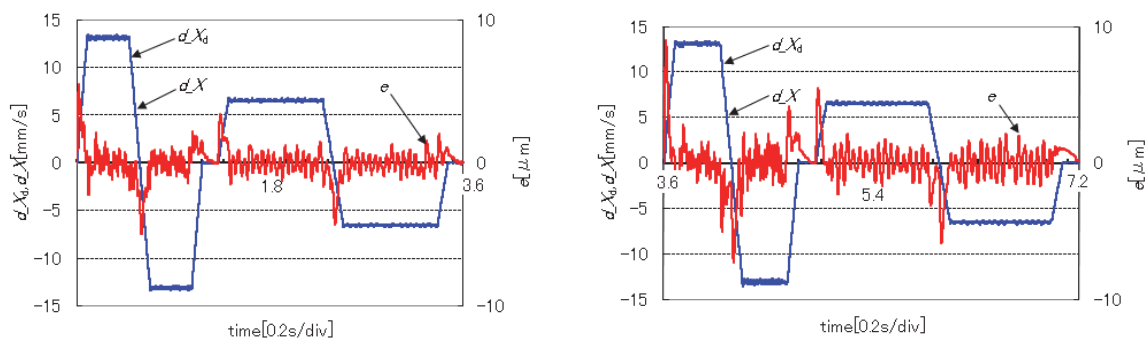

Fig. 12. The experimental results of tracking control using conventional control method. (left side: without weight, right side: with 5kg weight)
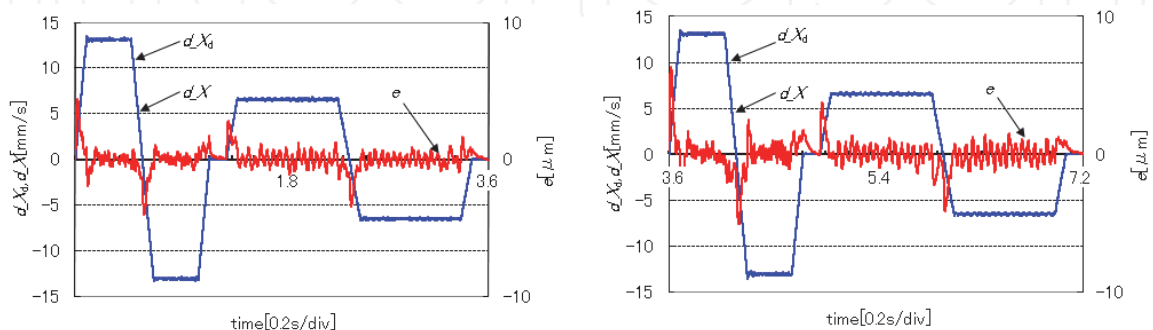

Fig. 13. The experimental results of tracking control using the proposed control method. (left side: without weight, right side: with 5kg weight)

Also, there was an error having to do with a ripple under constant velocity. The comparison results of tracking errors are shown in Table 1. It is obvious that the proposed method remains robust under controllability with or without the weight in the case of low-changing load conditions.

	tracking error[um]		
	start time	constant velocity	stroke end
conventional control without weight	+5.4	Max: +1.4 Min: −1.1	−4.8
conventional control with weight	+8.7	Max: +2.2 Min: −2.1	−7.0
proposed control without weight	+4.2	Max: +1.0 Min: −1.0	−4.0
proposed control with weight	+6.3	Max: +1.2 Min: −1.3	−4.9

Table 1. The comparison results of tracking errors.

3.2 A table drive system using AC linear motor
Next, we evaluated a tracking response in the low speed using a table drive system driven a linear motor, and the resolution of this system is 10 nm. After having investigated friction characteristics of this system because it was easy to receive a bad influence of the friction at the low-velocity movement, we inspected the effect of the proposed method.

3.2.1 Experimental system
Fig. 14 shows the photograph of single axis slider and the experimental system shown in Fig. 15. It consists of the following: (i) a one-axis stage mechanism consisting of an AC linear coreless motor which has no cogging force, (ii) a rolling guide mechanism, (iii) a position-sensor (1pulse=10nm), (iv) two current amplifiers, and (v) a personal computer with the controller, a D/A board and a counter board. In a practical application, high precision positioning at a low velocity is required, but in general, it is well known that the conventional control methods can not accomplish such a requirement. Moreover, the tracking error becomes large at the end of a stroke because of the effect of a friction force.
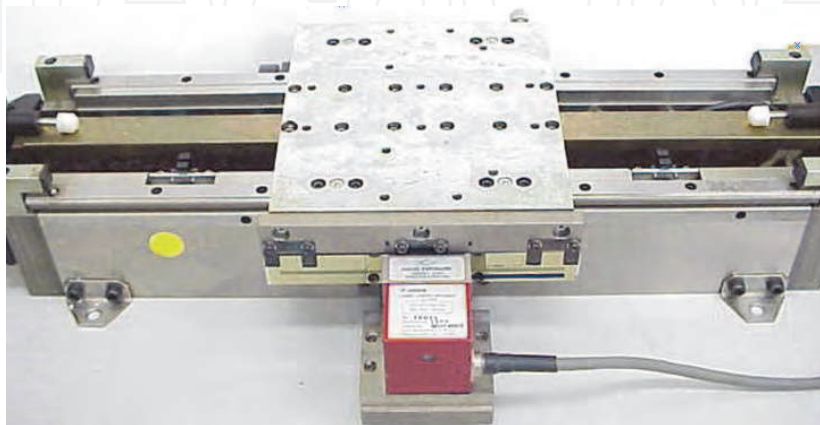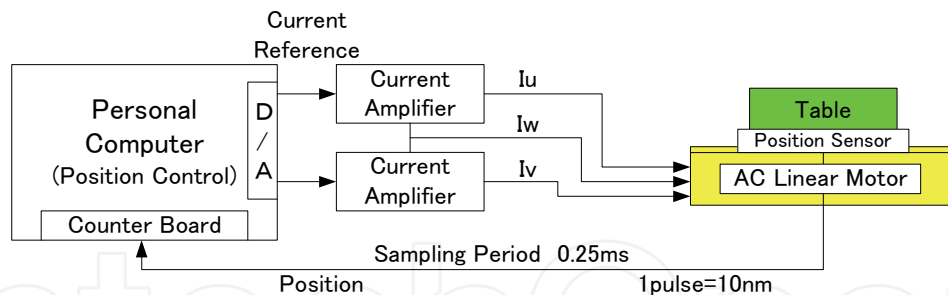

Fig. 14. The photograph of single axis slider.

Fig. 15. The experimental control system.

In the previous researches, a friction force can be regarded as a static function of velocity in spite of its complicated phenomenon. Therefore, the servo characteristics of this experimental system were investigated. Experiments have shown that there is a deflection or relative movement in the pre-sliding region, indicating that the relationship between the deflection and the input force resembles a non-linear spring with a hysteretic behavior. In this experiment, general PID control is used. Thus, the present study focuses on the nonlinear behavior at the end of a stroke during changes in velocity as shown in Fig. 16 (left side). In this figure, the signals of ①, ④ and ⑦ are velocity references, the signals of ②, ⑤ and ⑧ are velocity responses, the signals of ③, ⑥ and ⑨ are output forces with constant acceleration-deceleration profiles of 10 mm/s, 5.0 mm/s, and 2.5 mm/s, respectively. The forces in the actual experiment are calculated values and not the values actually measured. It seems that the tracking error of velocity are almost zero. From this figure, it is seen that the output forces are different during constant velocity and the force of 2.5 mm/s is the largest in all cases. The moving force generally needs a big one where velocity is large. The reason is influence of viscous friction. When the velocities are decreasing, output forces have not decreased and when the velocities are increasing, output forces have not increased.
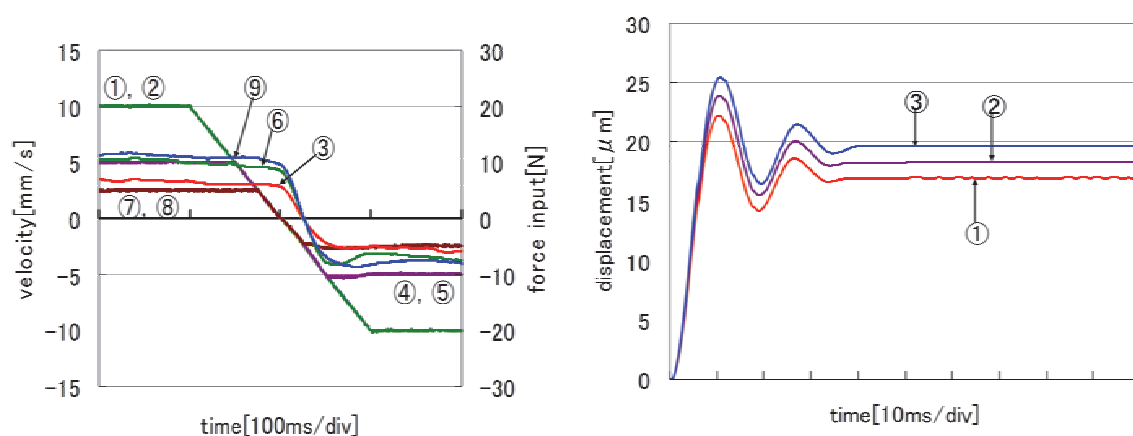

Fig. 16. The nonlinear behavior.
(left side: table motion at the end of a stroke, right side: spring-like behavior)

Further, when the output forces are set to zero, the spring- like behavior occurs at the end of a stroke, as shown in Fig.16 (right side). In this figure, the signals of ①, ② and ③ are the displacement, the command velocities which are 10 mm/s, 5.0 mm/s, and 2.5 mm/s,

respectively. At values of low command velocities, the spring-like behaviors produce large displacement. The displacement, which exceeds 15µm can negatively influence precision point to point control. The frequency of vibration was observed to be 40 Hz. The spring-like characteristic behavior is thought to be due to the elastic deformation between balls and rails in the ball guide-way. Thus, friction is a natural phenomenon that is quite hard to model description by on-line identification, and is not yet completely understood. Particularly, it is known to have a bad influence in a tracking response at the low-velocity movement. Next, in this table drive system with such a nonlinear characteristic, we evaluate the effectiveness of the proposed compensation method.
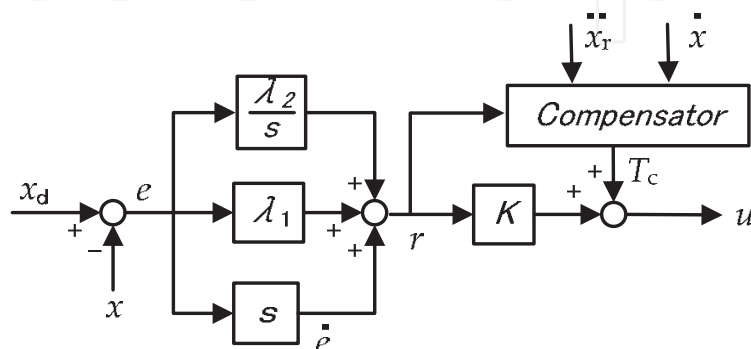

Fig. 17. The block diagram of the proposed method.

Fig. 17 shows a block diagram of the proposed control method, which consists of a PID controller (λ_1, λ_2, k), the proposed nonlinear compensator, T_c is disturbance compensation force. The control input u is given as follows

$$e = x_d - x \tag{19}$$

$$r = \dot{e} + \lambda_1 e + \lambda_2 \frac{e}{s} \tag{20}$$

$$\dot{x}_r = \dot{x}_d + \lambda_1 e + \lambda_2 \frac{e}{s} \tag{21}$$

$$u = kr + \frac{r}{\delta + |r|}(M_{\max}|\ddot{x}_r| + D_{\max}|\dot{x}| + F_{\max}) \tag{22}$$

The PID controller is tuned using the normal procedure, where a signal x_d is input reference, a signal x is displacement, a signal e is tracking error and s means Laplace transfer operator.

3.2.2 Experimental results
To show the effectiveness of the proposed method, experiments were carried out. Digital implementation was assumed in experimental setup. The sampling time of experiments was 0.25 ms. Parameters of PID controller was chosen as λ_1=125[1/s], λ_2=5208[1/s], k=62.5[1/s]. These parameters are adjusted from the ideal values which is determined by the triple

multiple roots condition. Here, the force conversion fixed constant is included in K. The parameters of proposed method was chosen as same value of PID controller and was chosen as δ=0.5. The value of M_{max}, D_{max} and F_{max} were set as five times of M, D, F of the slide table which measured beforehand, respectively. To evaluate the tracking errors at the end of stroke, we used three kind of moving velocities. Figs. 18, 19, 20 show the comparison results of tracking errors in the case of state velocity are 10 mm/s, 5 mm/s, 2.5 mm/s, respectively. In these figures, ① is the velocity reference, ② is the velocity response without compensation, ③ is the same one with compensation, ④ is the tracking error without compensation, ⑤ is the same one with compensation, ⑥ is the force output without compensation, ⑦ is the same one with compensation, respectively.
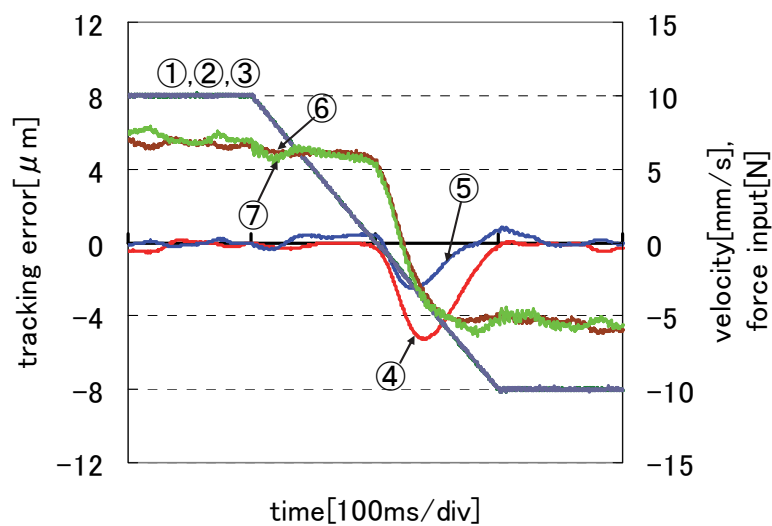

Fig. 18. The comparison results of tracking errors in the case of state velocity are 10mm/s.
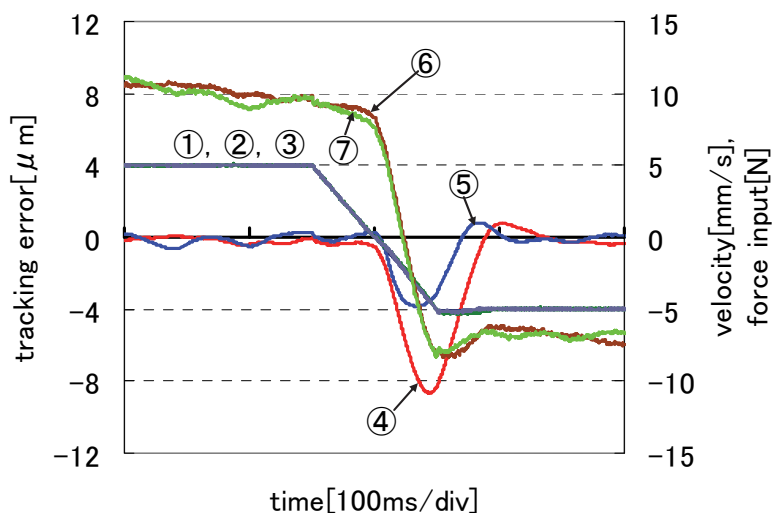

Fig. 19. The comparison results of tracking errors in the case of state velocity are 5mm/s.
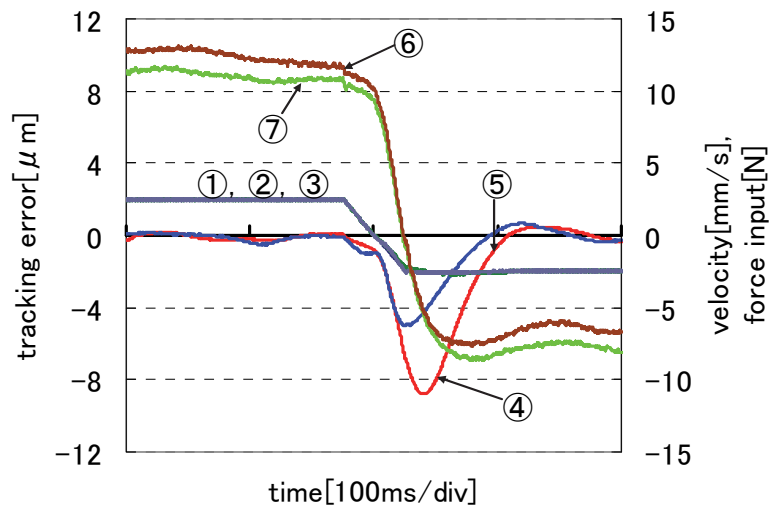
Fig. 20. The comparison results of tracking errors in the case of state velocity are 2.5mm/s.

Moving velocity	10mm/s	5mm/s	2.5mm/s
Without compensation	$-5.2\,\mu$m	$-8.6\,\mu$m	$-8.8\,\mu$m
With compensation	$-2.8\,\mu$m	$-3.8\,\mu$m	$-4.9\,\mu$m

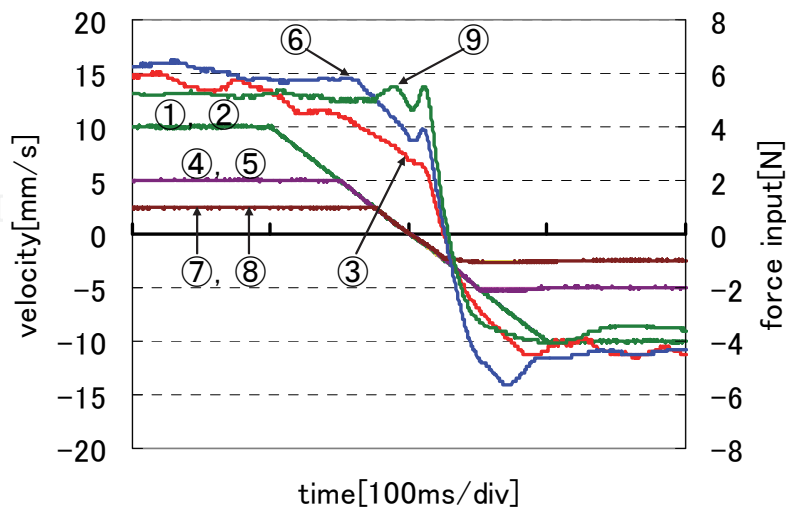Table 2. The comparison results of tracking errors.

Fig. 21. The compensate force inputs T_c among three cases of constant velocity.

It is obvious that the tracking errors of the case with compensation are reduced by more than 2/3 compared to the case of without compensation at the end of a stroke. Table 2 shows the tracking errors at the end of stroke. The errors are greatly reduced by our

proposed compensation method. Thus, the proposed method is judged to have better performance accuracy. Fig. 21 shows the compensate force inputs T_c among three cases of constant velocity. In Fig. 21, the signals of ①, ④ and ⑦ are velocity references, the signals of ②, ⑤ and ⑧ are velocity responses, the signals of ③, ⑥ and ⑨ are compensate forces of 10 mm/s, 5.0 mm/s, and 2.5 mm/s, respectively. It is clear that the compensation forces are similar to the nonlinear behaviors of Stribeck effect at the end of a stroke.

3.3 A table drive system using synchronous piezoelectric device driver

For the future applications of an electron beam (EB) apparatus for the semiconductor industry, a non-resonant ultrasonic motor is the most attractive device for a stage system instead of an electromagnetic motor, because the power source of the stage system is required for non-magnetic and vacuum applications. Next, we evaluated a stepping motion and tracking motion using a synchronous piezoelectric device driver.
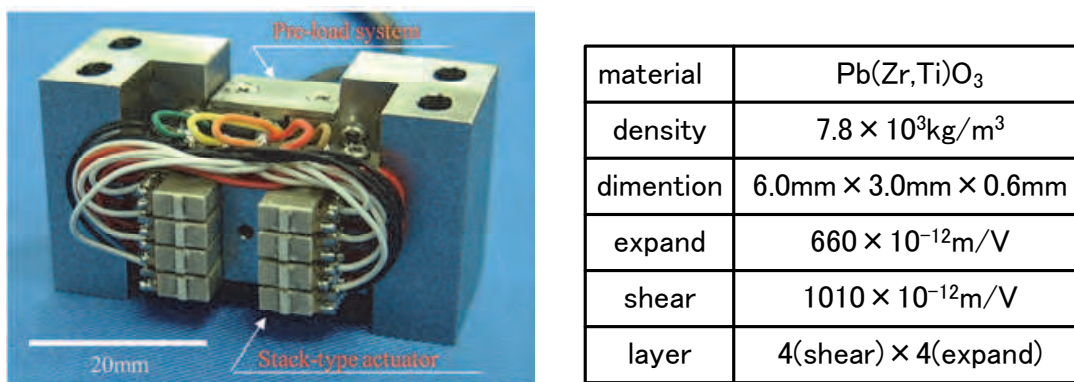

material	$Pb(Zr,Ti)O_3$
density	$7.8 \times 10^3 kg/m^3$
dimention	$6.0mm \times 3.0mm \times 0.6mm$
expand	$660 \times 10^{-12} m/V$
shear	$1010 \times 10^{-12} m/V$
layer	4(shear) × 4(expand)

Fig. 22. The photograph and specifications of SPIDER.

3.3.1 Experimental system

Fig. 22 shows a photograph of SPIDER (Synchronous Piezoelectric Device Driver) and its specifications. Fig. 23 shows the experimental setup which consists of the following parts. The control system was implemented using a Pentium IV PC with a DIO board and a counter board. The control input was calculated by the controller, and its value was translated into an appropriate input for the SPIDER through the DIO board , parallel-serial transfer unit, and drive unit. The position of the positioning table was measured by a position sensor with a resolution of 100 nm. The sensor's signal was provided as a feedback signal. The sampling period was 0.5 ms. The table was mounted on a driving rail. The weight of the moving part of the positioning table was approximately 1.2 kg. The friction tip was in contact with the side of the table. The longitudinal feed of the table was 100 mm. The positioning precision of this system depends on the resolution of the position sensor, and the best precision is less than 1 nm. The parallel-serial transfer unit translated the parallel data into serial data. The drive unit was a voltage generator for the piezoelectric actuator of SPIDER. Fig. 24 shows the motion of the SPIDER. The SPIDER has eight stacks and each stack consists of an extensible and shared piezoelectric element. The behavior of each stack is similar to that of a leg in ambulatory animals or human beings. Despite the limitation in the strokes of stack, the table can move endlessly. The motion sequence of the stacks is as follows (The sequence starts from the top of the left side. In this case, the table's direction of motion was to the right)
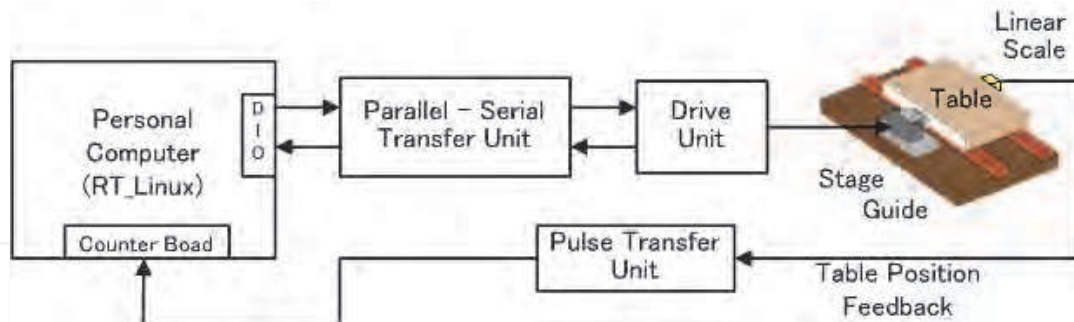
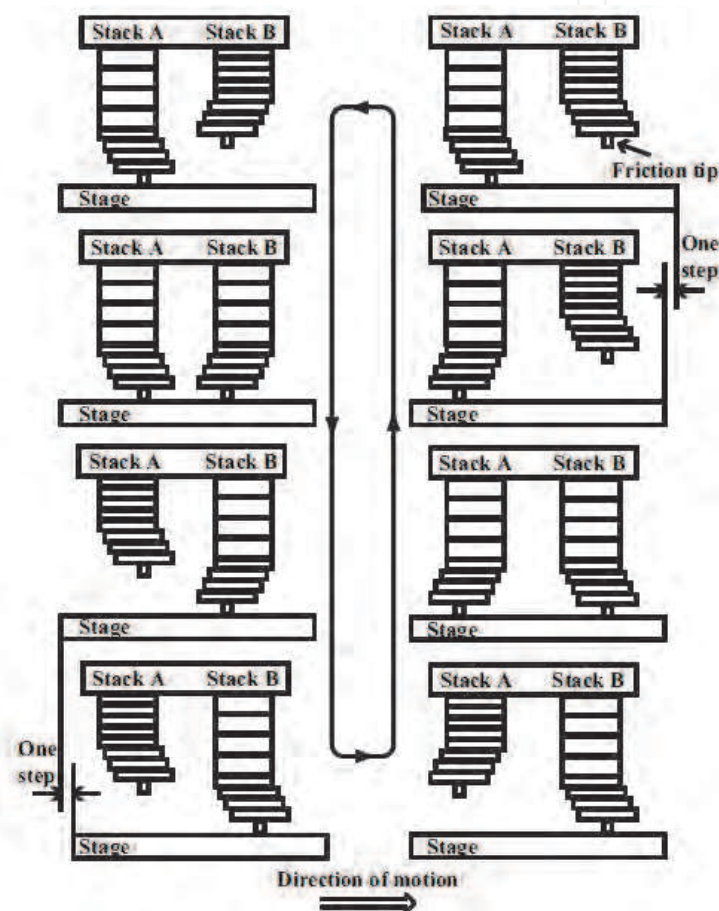Fig. 23. The experimental system for SPIDER.

Fig. 24. Operating sequence of SPIDER.

1. Deform stack B to the counter direction of the motion of the table;
2. Expand stack B to contact the stage;
3. Retract stack A;
4. Deform stack B to the forward direction of the motion of the table; then the stage move to the forward direction at one step;
5. Deform stack A to the counter direction of the motion of the table;
6. Expand stack A to contact the stage;
7. Retract stack B;
8. Deform stack A to the forward direction of the motion of the table; then the stage move in the forward direction in one step.

Continuous displacement of the positioning table can be given by repeating this sequence periodically. In addition, it is possible to be fast at speed of the motion of positioning table by increasing the amplitude of frequency and/or the voltage of this period. As we can see the positioning table is driven by the scratching and friction force via the SPIDER system. However, it is known that friction causes stick slip behavior; therefore, the frictional force is a major problem in precision positioning systems.

Next, we observe the nonlinear characteristic of the SPIDER system. To investigate the nonlinear characteristic of the SPIDER system, the open-loop control responses are measured. Fig. 25 shows the control input *u*; Fig. 26 shows the experimental open-loop responses of the positioning table displacement. These responses are measured five times. As we can see in Fig. 26, despite increasing the control input, the positioning table did not move during 0.2 seconds. Then we can regard that the SPIDER system exhibits time-delay phenomena. Fig. 27 shows the control input versus the displacement of the positioning table. As we can see in Fig.27, despite the control input being monotonically increasing / decreasing between a negative and positive value with equal magnitude, the displacement of positioning table shows strong hysteresis characteristics. Therefore, it seems that this SPIDER system can be regarded as a nonlinear system and it is very difficult to control the displacement of positioning table using only a linear control strategy. It is known that the deteriorating influence of friction is a major problem in many precision positioning systems. To remove as much of influence of friction as possible is very important.

Next, we applied our proposed control method with the nonlinear compensator for this system and inspected the effect of the method. First, the results of stepping motion which is one pulse motion are described. Secondly, the results of tracking motion of which amplitude of position references are 1 mm and 10 mm are described.
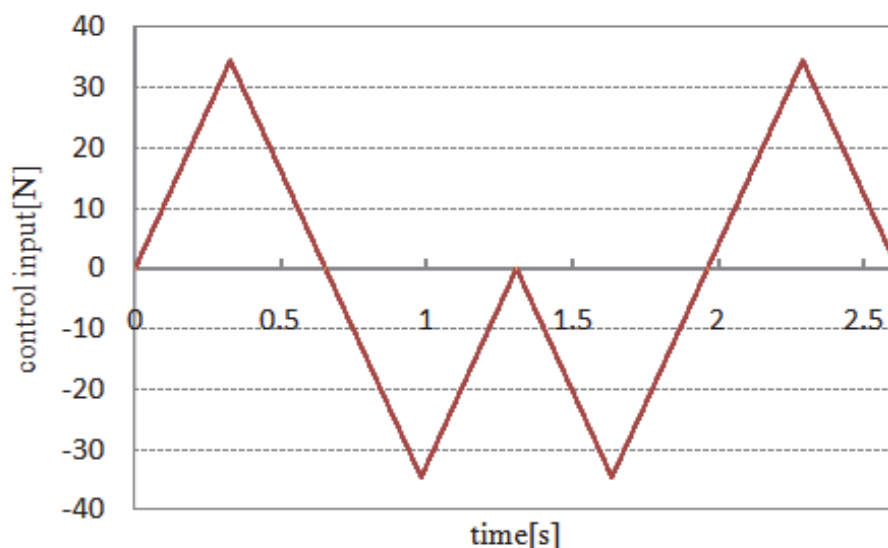

Fig. 25. The control input (0N→32N→0N→-32N→0N→-32N→0N→32N→0N).
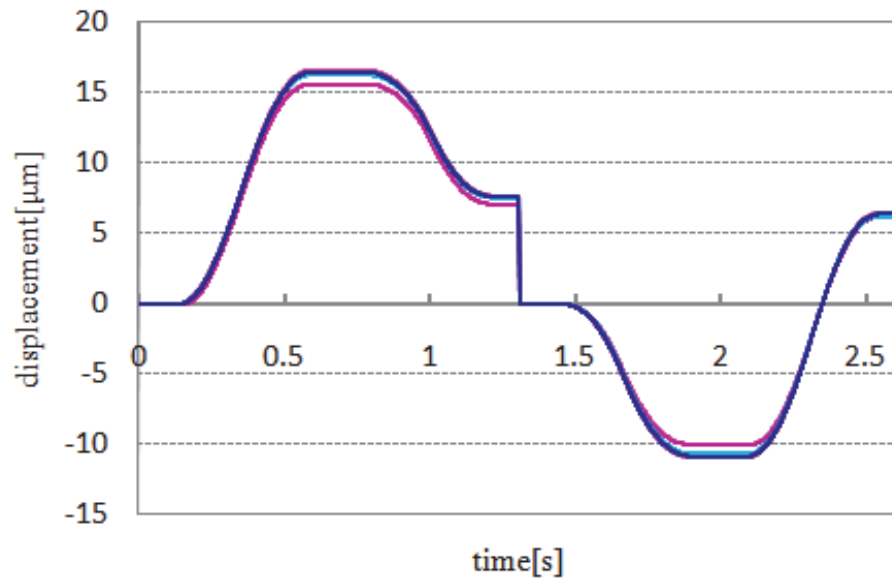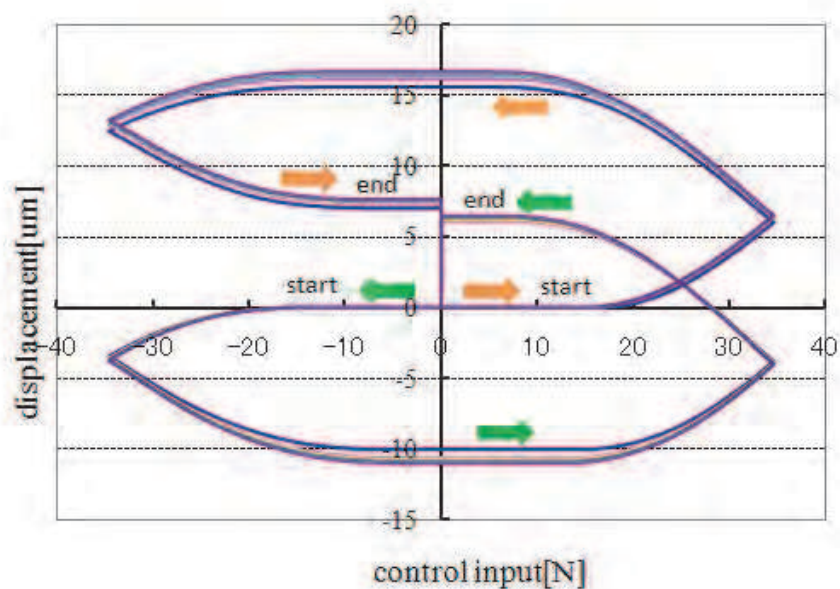
Fig. 26. The open-loop responses of SPIDER.

Fig. 27. The hysteresis characteristics of SPIDER.

3.3.2 Experimental results

To show the effectiveness of the proposed method, experiments were carried out. Fig. 28 shows a block diagram of the P,PI/I-P+FF control method with proposed compensator. Digital implementation was assumed in experimental setup. The sampling time of experiments was 0.5 ms. Parameters of P,PI/I-P+FF controller was chosen as in Table 3. The value of M_{max}, D_{max} and F_{max} were set as five times of M, D, F of the slide table which measured beforehand, respectively. The control input u is calculated as follows

$$e_1 = x_d - x \tag{23}$$

$$e_2 = K_p e_1 - \dot{x} + \alpha \dot{x}_d \tag{24}$$

$$r = K_v \left\{ \left(1 + \frac{K_i}{s} \right) e_2 - \beta \left(K_p e_1 + \alpha \dot{x}_d \right) \right\} \tag{25}$$

$$\ddot{x}_r = \alpha \ddot{x}_d (1 - \beta) + K_p \dot{e}_1 (1 - \beta) + K_i e_2 \tag{26}$$

$$T_c = \frac{r}{\delta + |r|} \left(M_{\max} |\ddot{x}_r| + D_{\max} |\dot{x}| + F_{\max} \right) \tag{27}$$

$$u = K_f r + T_c \tag{28}$$

To evaluate the proposed control method, the two position references were applied. First, the experimental results of stepping motion using conventional P,PI/I-P+FF control and proposed control are shown in Fig. 29. In the figure, ① is the position reference, ② is the table displacement and ③ is the positioning error. It is obvious that the positioning errors are greatly reduced using proposed control method compared to the conventional control
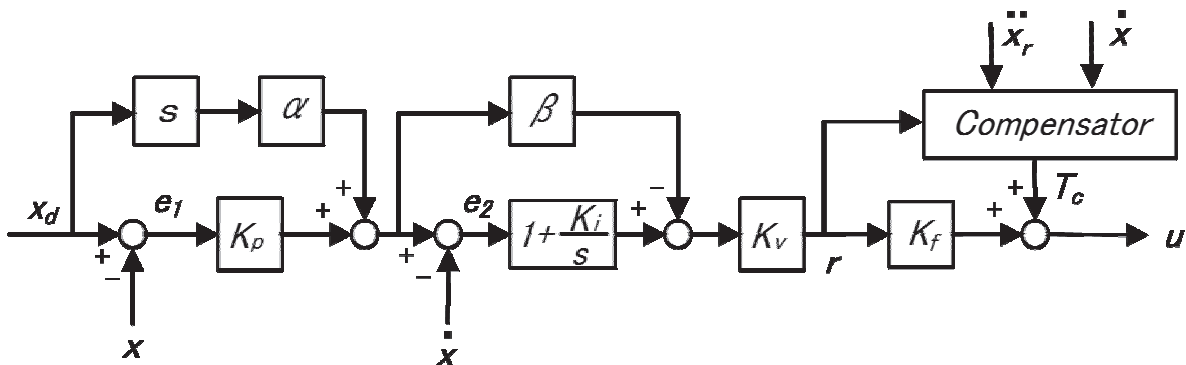

Fig. 28. Block diagram of the proposed control method.

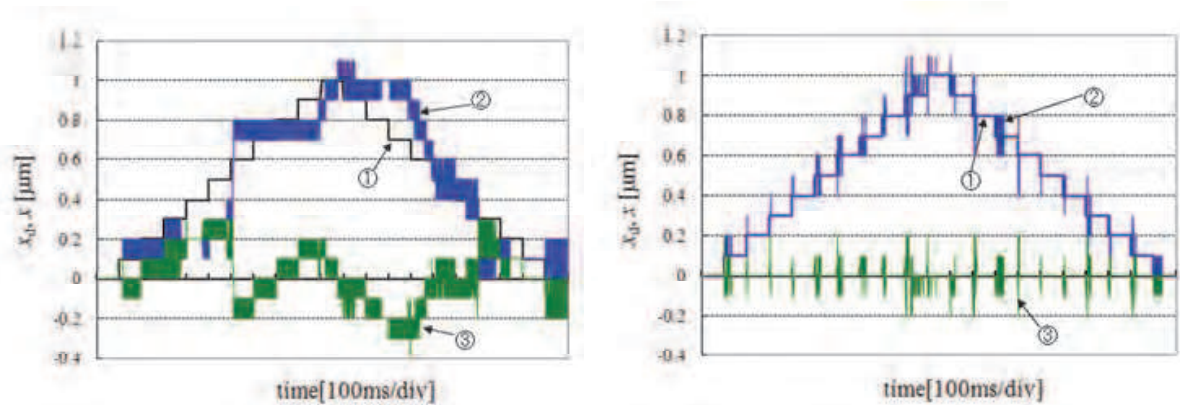|	
Position loop gain K_p	30[1/s]
Velocity loop gain K_v	188[1/s]
Velocity integral gain K_i	200[1/s]
Velocity feed-forward gain α	1.0
PI/I-P change constant β	0.0
Force constant K_f	946.2[1/N]
Maximum Mass constant M_{max}	6.0[kg]
Maximum viscous coefficient D_{max}	50[Ns/m]
Maximum disturbance constant F_{max}	48[N]
Chattering reject constant δ	1000

Table 3. Setting parameters of SPIDER.

Fig. 29. The experimental results of stepping motion.
(left side: conventional control, right side: proposed control)

method. Note, because the resolution of the position sensor is 100 nm by this experiment, the positioning resolution becomes 100 nm, but can raise positioning resolution to 0.6 nm if we improve the resolution of the position sensor. Secondly, Figs. 30, 31 showed the results of tracking motion of which amplitude of position references was 1 mm or 10 mm. In Figs. 30, 31, ① is the position reference, ② is the stage displacement and ③ is the tracking error, respectively. In these figures, the tracking errors of stroke end of the stage were expanded. Compared to each response, the results of proposed control were slightly improved to the results of conventional control. In order to investigate these results, the force input of the conventional control and proposed control were shown in Fig. 32. Both force inputs had a lot of vibrations to compensate undesired friction. In conventional control, the tracking error of stroke end was changed slowly in Fig. 32 (left side). On the other hand, in proposed control, the tracking error of stroke end was tracked to zero roughly in Fig. 32 (right side). Compared to these force inputs, the force input of proposed control was quickly and smoothly changed at the marked point. Therefore, we considered the tracking error of the proposed control method was improved.
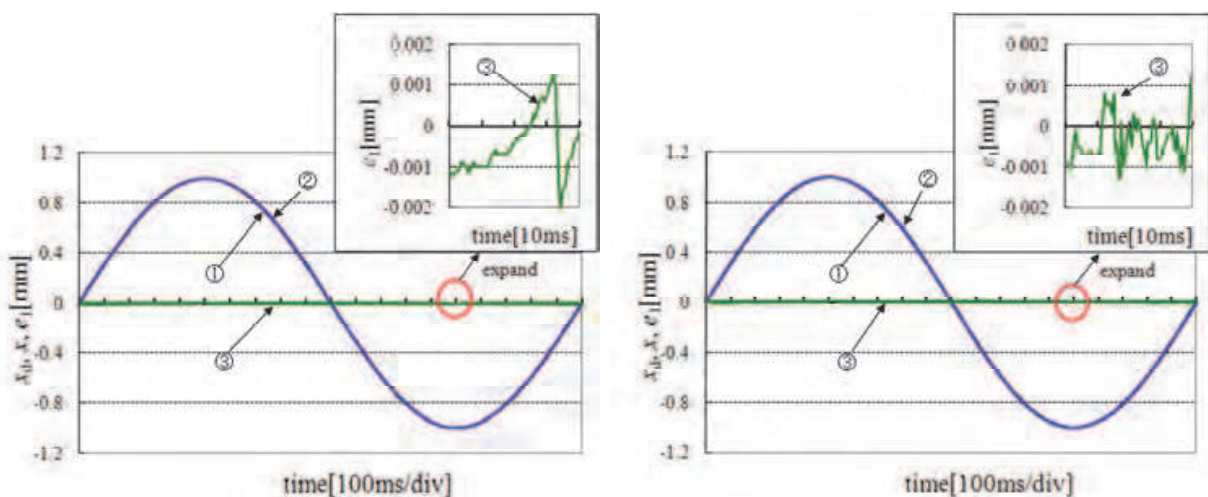

Fig. 30. The experimental results of tracking motion with 1mm moving.
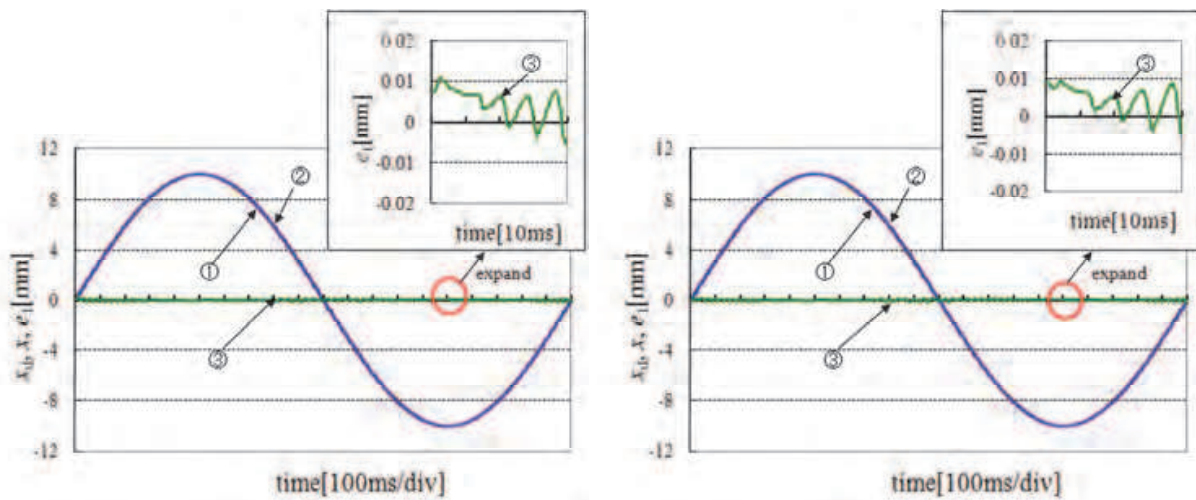(left side: conventional control, right side: proposed control)

Fig. 31. The experimental results of tracking motion with 10mm moving.
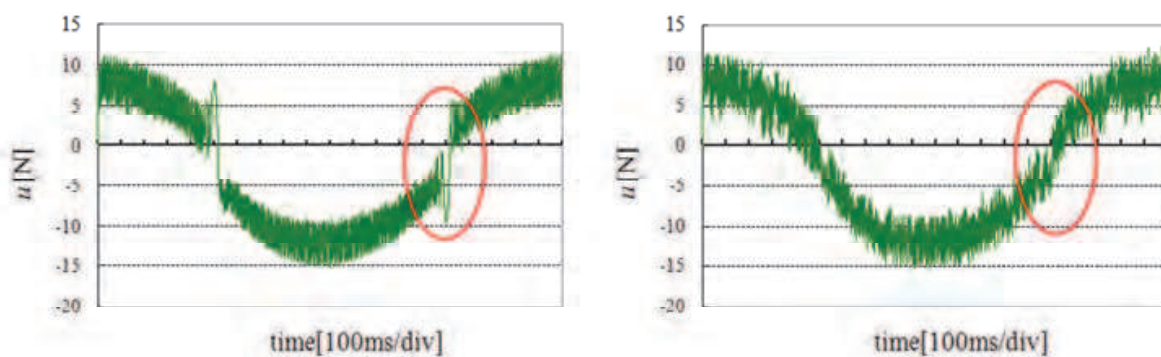(left side: conventional control, right side: proposed control)

Fig. 32. The force input of tracking motion with 1mm moving.
(left side: conventional control, right side: proposed control)

4. Conclusion

In this chapter, we propose a new PID control method that includes a nonlinear compensator that it is easy to understand for a PID control designer. The algorithm of the nonlinear compensator is based on sliding mode control with chattering compensation. The effect of the proposed control method is evaluated with three kinds of single-axis slide system experimentally. The first experiment system is two slider tables comprised of an AC servo motor, a coupling and a ball-screw, and the second one is a slide table using an AC linear motor and the third one is a slide table using synchronous piezoelectric device driver. By the first experiments, it is evaluated using single-axis slide system comprised of full closed feedback via point-to-point control response and tracking control response when load characteristics of the control target change. The experimental results indicate that the proposed control method has robustness in a high-speed, high-precision positioning response and a low speed tracking response when acceleration/deceleration of position reference change or the load characteristics of the control target change. By the second experiments, it is evaluated using a linear motor driven slider system via tracking control at

low-velocity, and the resolution of this system is 10nm. The tracking error of our proposed control method is reduced by more than 2/3 compared to the case of the conventional PID control method at the end of a stroke. By the third experiments, it is evaluated a stepping motion and trajectory tracking motion using a synchronous piezoelectric device driver. The positioning error of our proposed control is reduced by more than 2/3 compared to the case of the conventional PID control at a stepping motion.

Future studies will address the robustness and the control parameters tuning of the proposed compensation method. Furthermore, we want to evaluate the proposed method at an industrial robot used in a car assembly line and a twin linear drive table used in a semiconductor production device.

5. Acknowledgement

6. References

Canudas-de-Wit, C. Olsson, H. Astrom-K, J. & Lischinsky, P. (1995). A New Model for Control of System with Friction, *IEEE transaction on automatic control*, Vol.40, No.3, pp.419-425

Egashira, Y. Kosaka, K. Iwabuchi, T. Kosaka, T. Baba, T. Endo, T. Hashiguchi, H. Harada, T. Nagamoto, K. Watanabe, M. Yamakawa, T. Miyata, N. Moriyama, S. Morizono, Y. Nakada, A. Kubota, H. & Ohmi, T. (2002). Sub-Nanometer Resolution Ultrasonic Motor for 300mm Wafer Lithography Precision Stage, *Japanese Journal of Applied Physics*, vol.41, no.9, pp.5858-5863

Fujimoto, T. Tsuruta, K. & Uchida, Y. (2006). Motion Control of a Ball-Screw Slide System Via Multi-segment Sliding Mode Control Method, *Proceedings of the 8th MOVIC*, pp.842-847

Futami, S. Furutani, A. & Yoshida, S. (1990). Nanometer positioning and its microdynamics, *Nanotechnology*, 1, pp.31-37

Harashima, F. & Hashimoto,H. (1986). Sliding Mode Control, *Computorol*, No.13, pp.72-78.

Iwasaki, M. Shibata, T. & Matsui, N. (2000). GMDH-Based Autonomous Modeling and Compensation for Nonlinear Frication in Table Drive System, *IEEJ transaction*, vol.120-C, no.1, 2000, pp.20-26

Kojima, T. (2004). Robot Control, *published by Corona co.jp*

Kosaka, K. Iwabuchi, T. Baba, T. Endo, T. Hashiguchi, Furukawa, H. Egashira, Y. Hashimoto, S. Touge, M, Uozumi, K. Nakada, A. Kubota, H. & Ohmi, T. (2006)."Wear Reduction Method for Frictionally Fast Feeding Piezoactuator, *Japanese Journal of Applied Physics*, vol.45, no.2A, pp.1005-1011

Kuwon, T. Sul, S. Nakamura, H. & Tsuruta, K. (2006). Identification of Mechanical Parameters for Servo Drive, *Proceedings of the IEEE/IAS 41st Annual meeting*, IAS22p4, Florida, USA

Lischinsky, P. Canudas-de-Wit, C. Morel, & G. (1999). Friction compensation for an Industrial Hydraulic Robot, *IEEE Control Systems*, Februaly, pp.25-32

Nonami, K. & Den, H. (1994). Sliding Mode Control, *published by Corona co.jp*

Otsuka, J. & Masuda, T. (1998). The influence of nonlinear spring behavior of rolling elements on ultra-precision positioning control systems, *Nanotechnology*, 9, pp.85-92

Sato, K. Tsuruta, K. & Ishibe, T. (2007). A Design of Adaptive Control for Systems with Input Nonlinearities and Its Experimental Evaluations, *T.SICE*, Vol.43, No.3, pp.221-226.

Sato, K. Tsuruta, K. & Shoji, A. (2005). Adaptive Friction Compensation Control of Linear Slider with Considering a Periodic Reference Signal, *IEEJ Transactions on Industry Applications*, Vol.125, No.11, pp.1022-1029

Sato, K. Tsuruta, K. & Mukai, H. (2007). A robust adaptive control for robotic manipulator with input torque uncertainty, *Proceedings of the SICE Annual Conference 2007*, Sept. 17-20, pp1293-1298

Sato, K. Ishibe, T. Tsuruta, K. (2007). A design of adaptive H∞ control for positioning mechanism system with input nonlinearities, *Proceedings of the 16th IEEE International Conference on Control Applications Part of IEEE Multi-conference on Systems and Control*, pp.152-157

Sato, K. Nishijima, D. Tsuruta, K. (2006). Adaptive H∞ control method with frictions compensation and disturbance rejection for robotic manipulators, *Proceedings of the IEEE International Conference on Control Applications*, pp.1031-1036

Sato, K. Mukai, H. & Tsuruta, K. (2008). An adaptive H∞ control for robotic manipulator with compensation of input torque uncertainty, *Preprints of the 17th IFAC World Congress*, pp. 8919-8924

Suzuki, T. (2001). Adaptive Control, *published by Corona.co.jp*

Tsuruta, K. Murakami, T. Futami, S. & Sumimoto, T. (2000). Genetic Algorithm (GA) Based Modeling of Non-linear Behavior of Friction of a Ball Guide Way, *Proceedings of the 6th International Workshop on Advanced Motion Control*, pp.181-186

Tsuruta, K. Murakami, T. & Futami, S. (2000). Nonlinear Frictional Behavior at Low Speed in a Ball Guide Way, *Proceedings of the International Tribology Conference Nagasaki 2000*, pp1847-1852

Tsuruta, K. Murakami, T. & Futami, S. (2003). Nonlinear Friction Behavior of Discontinuity at Stroke End in a Ball Guide Way, *Journal of the Japan Society for Precision Engineering*,Vol.69,No.12, pp.1759-1763

Tsuruta, K. Sato, K. Ushimi, N. & Fujimoto, T. (2007). High Precision Positioning Control for Table Drive System using PID Controller with Nonlinear Friction Compensator, *Proceedings of the 4th International Conference on Leading Edge Manufacturing in 21st Century Fukuoka*, pp.173-176

Tsuruta, K. Sato, Sawada, S. Kosaka, K. & Schilling, K. (2007). A Comparison of Nonlinear Friction Compensations for a High Precision Stage using Synchronous Piezoelectric Device Driver, *Asian Symposium for Precision Engineering and Nanotechnology 2009*, 1E-10-2191

Utkin, V, I. (1977). Variable Structure Systems with Sliding Mode, *IEEE Transaction on Automatic Control*, Vol.AC-22, pp.212-222
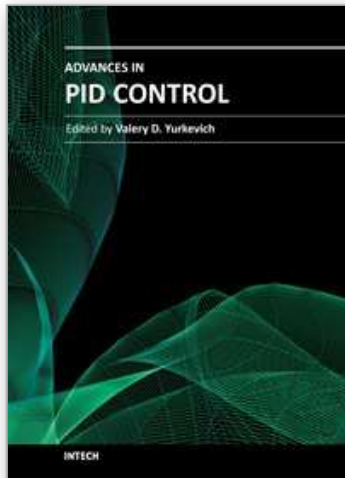
Advances in PID Control

Edited by Dr. Valery D. Yurkevich

Since the foundation and up to the current state-of-the-art in control engineering, the problems of PID control steadily attract great attention of numerous researchers and remain inexhaustible source of new ideas for process of control system design and industrial applications. PID control effectiveness is usually caused by the nature of dynamical processes, conditioned that the majority of the industrial dynamical processes are well described by simple dynamic model of the first or second order. The efficacy of PID controllers vastly falls in case of complicated dynamics, nonlinearities, and varying parameters of the plant. This gives a pulse to further researches in the field of PID control. Consequently, the problems of advanced PID control system design methodologies, rules of adaptive PID control, self-tuning procedures, and particularly robustness and transient performance for nonlinear systems, still remain as the areas of the lively interests for many scientists and researchers at the present time. The recent research results presented in this book provide new ideas for improved performance of PID control applications.

How to reference

In order to correctly reference this scholarly work, feel free to copy and paste the following:

Kazuhiro Tsuruta, Kazuya Sato and Takashi Fujimoto (2011). High-Speed and High-Precision Position Control Using a Nonlinear Compensator, Advances in PID Control, Dr. Valery D. Yurkevich (Ed.), ISBN: 978-953-307-267-8, InTech, Available from: http://www.intechopen.com/books/advances-in-pid-control/high-speed-and-high-precision-position-control-using-a-nonlinear-compensator